PAPER

Selective enhancement of auxeticity through changing a diameter of nanochannels in Yukawa systems

IOP Publishing Smart Materials and Structures
Smart Mater. Struct. 27 (2018) 115021 (8pp) https://doi.org/10.1088/1361-665X/aae6a4

Selective enhancement of auxeticity through changing a diameter of nanochannels in Yukawa systems

Konstantin V Tretiakov, Paweł M Pigłowski, Jakub W Narojczyk and Krzysztof W Wojciechowski

Institute of Molecular Physics, Polish Academy of Sciences, Smoluchowskiego 17, 60-179 Poznań, Poland

E-mail: tretiakov@ifmpan.poznan.pl

Received 25 July 2018, revised 18 September 2018
Accepted for publication 8 October 2018
Published 23 October 2018

Abstract

A new effect of selective enhancement of auxeticity through the changes of nanochannels' diameter in Yukawa systems is reported. Elastic properties of the model of Yukawa crystals with narrow nanochannels in the [001] crystallographic direction have been studied by Monte Carlo simulations in the isobaric–isothermal ensemble. It has been found that the choice of nanochannels' diameter allows one to decrease the Poissons ratio value of the system in one of two selected crystallographic directions. The value of Poisson's ratio in those directions can be changed in a wide range, e.g. from $-0.061(9)$ to $-0.625(44)$ in the $[011][01\bar{1}]$-direction, depending on the nanochannels' type and the Debye screening length.

Keywords: auxetics, negative Poisson's ratio, nanochannels, Yukawa potential, Monte Carlo simulations

(Some figures may appear in colour only in the online journal)

1. Introduction

Auxetics [1, 2] belong to the class of smart materials [3–12] because of their extraordinary and counterintuitive elastic properties. They increase lateral dimensions in process of stretching and decrease lateral dimensions under compressing. This unique property is described by the Poisson's ratio [13], which becomes negative in the case of auxetic systems. Auxetic materials and models describing their properties undergo intensive research not only in the scope of basic research [14–16], but also from the perspective of possible applications [17–21]. Besides the search for auxetic properties in various homogeneous materials and models [22–38], in recent years the seek for auxetic properties in heterogeneous systems like hybrid materials or composites, became particularly interesting and important. Is it worth to note, that these research are conducted both at macro [39–45] and micro scale [46–56]. Based on models that explain the origin of auxetic properties [35, 39, 46, 57–63] attempts are taken to create composites exhibiting the negative Poisson's ratio [64–67]. Moreover, novel materials are thoroughly examined for exhibiting auxetic properties [68, 69]. An example of such materials are colloidal crystals [70, 71]. They are interesting from the practical applications perspective [72–75] and, as it has been shown recently, they exhibit auxetic properties [76]. Recent studies revealed a significant influence of particle's size polydispersity on auxetic properties in such systems [54]. Furthermore, models of colloidal crystals became the subject of study in order to determine how the structural modifications drive the changes in elastic properties [50, 51, 54, 55]. In other words, there are attempts to create heterogeneous model systems at micro scale—nanocomposites. The idea for such model systems emerges from the fact that some physical properties of charge stabilized colloids [77–83] can be very accurately approximated with the use of hard-core repulsive Yukawa pair potential (HCRYP) [77–79, 81]:

$$\beta u_{ij} = \begin{cases} \infty, & r_{ij} < \sigma, \\ \beta\epsilon \dfrac{\exp[-\kappa\sigma(r_{ij}/\sigma - 1)]}{r_{ij}/\sigma}, & r_{ij} \geqslant \sigma, \end{cases} \quad (1)$$

where: $\beta = \frac{1}{k_B T}$, k_B is the Boltzmann constant, T is the temperature, σ is the diameter of the particles' hard core, ϵ is

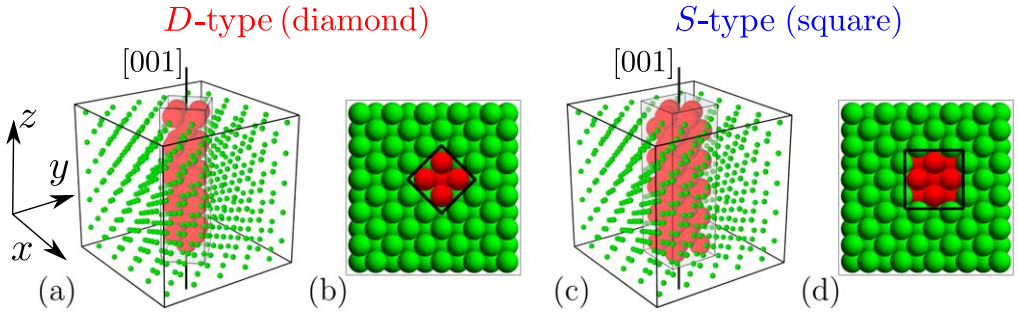

Figure 1. The structures of studied systems with nanochannels in the [001]-crystallographic direction: (a), (b) the nanochannel of D-type; (c), (d) the nanochannel of S-type. By green and red colors are marked Yukawa particles and hard spheres, respectively. In figures (a) and (c), the centers of Yukawa particles are marked by green dots in order to better illustrate the structure of the nanochannel created by hard spheres. Figures (b) and (d) represent the projections of systems on the *XY* plane.

the contact potential, κ is the inverse of the Debye screening length and r_{ij} is the distance between the centers of i and j particles. As was mentioned above, earlier research showed that a charge stabilized colloidal crystal modeled as a set of particles interacting with hard-core Yukawa potential does exhibit auxetic properties [76]. The latter are enhanced by the increasing polydispersity of particle sizes [54]. On the other hand, if some of the particles lack charge, they can be described with hard interactions:

$$\beta u_{ij} = \begin{cases} \infty, & r_{ij} < \sigma, \\ 0, & r_{ij} \geqslant \sigma. \end{cases} \tag{2}$$

In other words, a subset of the model particles can interact with other particles only with the hard potential, i.e. without the part modeling the averaged electrostatic interactions. Thus, one obtains a heterogeneous model where particles interacting only with hard potential may be regarded as inclusions. A recent study of such systems with inclusions in the form of nanochannels (or nanorods) or nanoslits (or nanolayers) revealed that the introduction of hard inclusions to fcc crystal of Yukawa particles induces [51, 55] or enhances [50, 54] auxetic properties. Instead, the results presented in this work show that, in the case of systems with nanochannels, the diameter of the latter ones has a significant impact on auxetic properties as well. The change of the nanochannel diameter allows one for selective modification of the Poisson's ratio value in selected crystallographic direction. In particular, we present an idea of possible structural modifications and test them in a model system which is close to real colloidal systems in which charge, size and shape of particles can be changed [79, 81, 83–85]. We can add that recent experiments by Demirörs *et al* illustrate the approach producing single-component and multicomponent colloidal arrays in complex three-dimensional structures [86]. So, we believe that a rapid progress in the nanotechnology observed in the last years should lead in a near future to creation of methods which will allow one to perform structural modifications described in the paper.

The main goal of this work is to demonstrate strong influence of the hard-sphere-nanochannels' diameter on auxetic properties of the considered model material. In this paper, we show a new possibility to tune the values of Poissons ratio depending on the type (diameter) of the channel that can help in designing composites with desired properties (not only at nanoscale), e.g. in the case when a huge enhancement of auxeticity in given direction is required.

The paper is organized in the following way. In the next section the details of the model and methods used have been presented. In section 3 analysis and discussion of the obtained results have been provided. Summary and conclusions in section 4 complete the paper.

2. Model and method

2.1. Model

The studied model consists of N particles forming the face-centered cubic (fcc) lattice at close packing. Part of the particles (further called Yukawa particles) forming the bulk of the system, interacts via the HCRYP (equation (1)). The remaining particles (further referred to as hard spheres) constitute an inclusion in a form of a nanochannel. More precisely, they create an array of inclusions due to periodic boundaries which are applied in the studied model. Hard spheres form nanochannels along axis in the [001]-crystallographic direction (see figure 1), and interact with all the particles in the system through the hard potential (equation (2)). Typical super-cells of the studied model are presented in figures 1(a) and (c).

In order to perform quantitative analysis of the influence of various inclusions on elastic properties, we introduce a parameter which measures the concentration of the inclusion particles in the system:

$$c = \frac{N_{\mathrm{HS}}}{N} \times 100\%, \tag{3}$$

where N_{HS} is the number of hard spheres forming the nanochannel (inclusion).

In the present paper two types of the channels with different diameters are considered. The first narrower channel, with the diameter equal to $\sqrt{2}\sigma$ is further referenced to as D-type channel (see figure 1(a)). The second channel with the diameter equal to 2σ is further referenced to as S-type channel (see figure 1(c)). The concentration of channel particles of

Table 1. Concentration of hard spheres (see equation (3)) in studied systems with respect to their size and the type of the channel.

	D-type		S-type	
N	N_{HS}	c	N_{HS}	c
256	20	7.8125%	—	—
500	25	5.0000%	45	9.0000%
864	30	3.4722%	54	6.2500%
1372	35	2.5510%	63	4.5918%
2048	40	1.9531%	72	3.5156%

each type was varied by changes of the system size. Details of the system sizes and corresponding them values of concentration are collected in table 1. The studies of size effect on the elastic properties of systems with nanochannels have been done in our previous work [50]. It has been found that the symmetry of the crystal and its stability are well approximated by samples constituted of single super-cells, i.e. with a single channel in the case of the studied type of the Yukawa systems. Based on this, in the present work the samples with a single nanochannel, which can be thought of as super-cells (figure 1), have been studied. The application of the periodic boundary conditions gives a periodic structure with parallel nanochannels.

2.2. Method

The model systems, described in the previous subsection, have been studied by Monte Carlo simulations in the *NpT*-ensemble, i.e. N particles at fixed pressure, p, and temperature, T. In order to evaluate the elastic properties of the system, the Parinello–Rahman method has been employed [87–89]. According to the Parinello–Rahman approach, the elastic compliance tensor S_{ijkl} (a fourth rank symmetric tensor) can be determined directly from the fluctuations of the strain tensor components $S_{ijkl} = \langle \Delta\varepsilon_{ij} \Delta\varepsilon_{kl} \rangle V_p / k_B T$, where $\varepsilon = (\mathbf{h}_0^{-1}.\mathbf{h}.\mathbf{h}.\mathbf{h}_0^{-1} - \mathbf{I})/2$ is the strain tensor, $\mathbf{h}$ is the simulation box matrix defined as:

$$\mathbf{h} = \begin{bmatrix} h_{11} & 0 & 0 \\ 0 & h_{22} & 0 \\ 0 & 0 & h_{33} \end{bmatrix}, \tag{4}$$

$\mathbf{h}_0$ is the reference box matrix. $\mathbf{I}$ is the 3×3 identity matrix. It is worth to note that $\mathbf{h}$ and $\mathbf{h}_0$ are symmetric.

In general, there could be 81 components of the fourth rank tensor like S_{ijkl}. However, due to the symmetry of the strain tensor ε, this value is reduced to not more than 21 independent components of the S_{ijkl}. With the latter ones one can fully describe the elastic properties of a crystal at arbitrary symmetry. The knowledge of the elastic compliance tensor allows one for direct calculations of the Poisson's ratio in any direction. The value of the Poisson's ratio is calculated from the formula [51, 90]:

$$\nu_{nm} = -\frac{m_i m_j S_{ijkl} n_k n_l}{n_p n_r S_{prst} n_s n_t} = -\frac{S_{nm}}{S_{nn}}, \tag{5}$$

where $\vec{\mathbf{n}}$ is the direction of the applied stress, $\vec{\mathbf{m}}$ is the direction of the system response on the applied deformation, and $\vec{\mathbf{n}} \cdot \vec{\mathbf{m}} = 0$. More details on the calculations of the elastic constants can be found in [50, 89].

In this paper we focus our attention on changing auxetic properties of the system induced by modifying the diameter of nanochannels. For this purpose, it is suitable to use the degree of axeticity which is defined in the following way [54]:

$$\chi = \sqrt[3]{\frac{3A}{4\pi}}, \tag{6}$$

where:

$$A = \int_0^{2\pi} \mathrm{d}\phi \int_0^{\pi} \sin\theta \mathrm{d}\theta \int_0^{R(\theta,\phi)} r^2 \mathrm{d}r, \tag{7}$$

and $R(\theta, \phi) = \frac{1}{2\pi} \int_0^{\pi} (|\nu_{n(\theta,\phi)}(\alpha)| - \nu_{n(\theta,\phi)}(\alpha)) \mathrm{d}\alpha$ can be thought of as the mean of negative values of Poisson's ratio corresponding to the direction of $\vec{\mathbf{n}}(\theta, \phi)$. Here, α is the angle between $\vec{\mathbf{m}}$ (the direction of measurement of the response) and the versor which is created by the cross section of the plane *OXY* and the plane orthogonal to versor $\vec{\mathbf{n}}$ (direction of applied stress). For more details, see [50, 54].

Elastic properties of Yukawa systems with different diameters of nanochannels were evaluated in a wide range of the inverse screening length ($8 \leqslant \kappa\sigma \leqslant 17$) for the contact potential $\beta\epsilon = 20$ and reduced pressure $p^* = \beta P \sigma^3 = 100$. The values of these parameters have been selected based on the analysis of results of previous works [50, 76, 81]. The cut-off radius equal to 2.5σ was used. Standard scheme for Monte Carlo simulations with two typical trial moves was employed [91] for which the acceptance ratio of box moves and particle moves was around 30%. Typical simulation run lasted at least 2×10^6 MC cycles after the system had reached the state of thermodynamic equilibrium (usually 10^6 MC cycles). All evaluated values, such as elastic compliances and the Poissons ratios, have been determined as the averages from 10 independent runs.

3. Results and discussion

Simulations of the system were started from perfect fcc structures with nanochannels. During about first thousand MC steps (figure 2(a)) the simulation box was changing its volume and shape, approaching the equilibrium state for which the box matrix takes the form:

$$\mathbf{h} = \begin{bmatrix} h_{11} & 0 & 0 \\ 0 & h_{11} & 0 \\ 0 & 0 & h_{33} \end{bmatrix}. \tag{8}$$

Analysis of the box matrix reveals that it is diagonal and defines a cuboid with the square base ($h_{11} = h_{22} \neq h_{33}$). So, the symmetry of the system with a [001] nanochannel (for both types of the channels) is tetragonal, what is reflected in

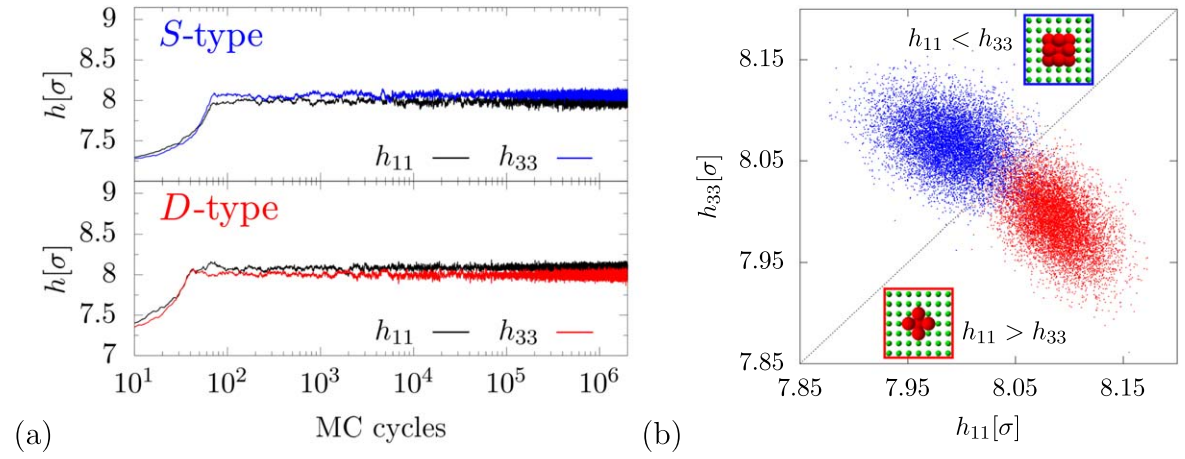

Figure 2. Components of the simulation box of system consisting of 500 particles at $\kappa\sigma = 10$, $\beta\epsilon = 20$. (a) Components h_{11} and h_{33} versus MC steps for both types of channels. (b) Dependence of the components of box matrix h_{33} versus h_{11} during MC simulations in thermodynamic equilibrium.

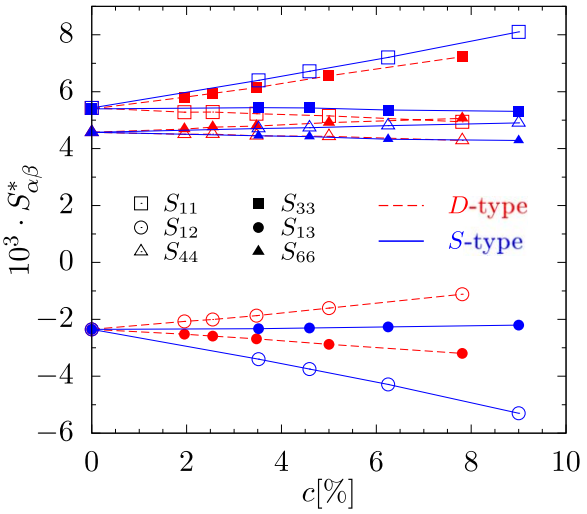

Figure 3. Elastic compliancies of Yukawa crystals with nanochannels as a function of concentration at $\kappa\sigma = 10$, $\beta\epsilon = 20$.

the following form of the compliance matrix:

$$\mathbf{S} = \begin{bmatrix} S_{11} & S_{12} & S_{13} & 0 & 0 & 0 \\ S_{12} & S_{11} & S_{13} & 0 & 0 & 0 \\ S_{13} & S_{13} & S_{33} & 0 & 0 & 0 \\ 0 & 0 & 0 & S_{44} & 0 & 0 \\ 0 & 0 & 0 & 0 & S_{44} & 0 \\ 0 & 0 & 0 & 0 & 0 & S_{66} \end{bmatrix}. \quad (9)$$

Furthermore, in figure 2(b) one can see that introduction of different types of nanochannel lead to change the relations between components of the box matrix. We observed that $h_{11} < h_{33}$ for systems with S-type channel, and $h_{11} > h_{33}$ for D-type systems. Consequently, we have the following relations between the elastic compliance elements depending on the type of the channel. We observed $S^*_{11} > S^*_{33}$, $S^*_{13} > S^*_{12}$, and $S^*_{44} > S^*_{66}$ for the S-type systems, whereas for the D-type systems these relations were $S^*_{11} < S^*_{33}$, $S^*_{13} < S^*_{12}$, and $S^*_{44} < S^*_{66}$. This is clearly seen in figure 3 which presents elastic compliance matrix elements of systems with nanochannels as a function of concentration of the 'channel' particles in the system. In addition, one can see there that an increase of concentration results in an enhancement of those relations.

The change of the diameter of nanochannels in Yukawa systems is more pronounced in the value of Poisson's ratio. In the figure 4 the Poisson's ratio values for auxetic directions ([110][1$\bar{1}$0] and [011][01$\bar{1}$]) with respect to concentration c are presented for various screening lengths. Here,we observe the possibility to selectively enhance or reduce the auxeticity in selected crystallographic direction. One can see that, depending on the type of the channel ('*D*' or '*S*'), one observes a strong decrease of the Poisson's ratio in one of the crystallographic directions: [110][1$\bar{1}$0] or [011][01$\bar{1}$] respectively,while simultaneously preserving auxetic properties in the other one. Thus,one can note that in the case of S-type channel an increase of concentration has no effect on the Poisson's ratio in the [110][1$\bar{1}$0]-direction regardless of the screening length (figure 4(a)). On the other hand,the value of Poisson's ratio in the [011][01$\bar{1}$]-direction for S-type systems decreases along with increasing concentration for all studied screening lengths. The most significant decrease of the Poisson's ratio from $-0.214(9)$ to $-0.625(44)$ at $c = 9\%$ and $\kappa\sigma = 8$ is observed (figure 4(b)). (The number in parentheses is the numerical value of the standard experimental error (uncertainty) referred to the corresponding last digits of the quoted result.) The opposite behavior of Poisson's ratio was found for nanochannels of D-type. In the [011][01$\bar{1}$]-direction the value of Poisson's ratio is almost constant for various concentrations (figure 4(b)). Minor decrease of the value of Poisson's ratio with an increase in c can be noticed for the shortest screening length (when $\kappa\sigma = 17$). In contrast,the Poisson's ratio in the [110][1$\bar{1}$0]-direction decreases with increasing concentration. The most significant decrease of ν can be observed for $\kappa\sigma = 8$ (figure 4(a)).

The possibility to selectively enhance or reduce of the auxetic properties depending on the diameter of nanochannel can be analyzed using the minimal negative value of the Poisson's ratio in all crystallographic directions. In the

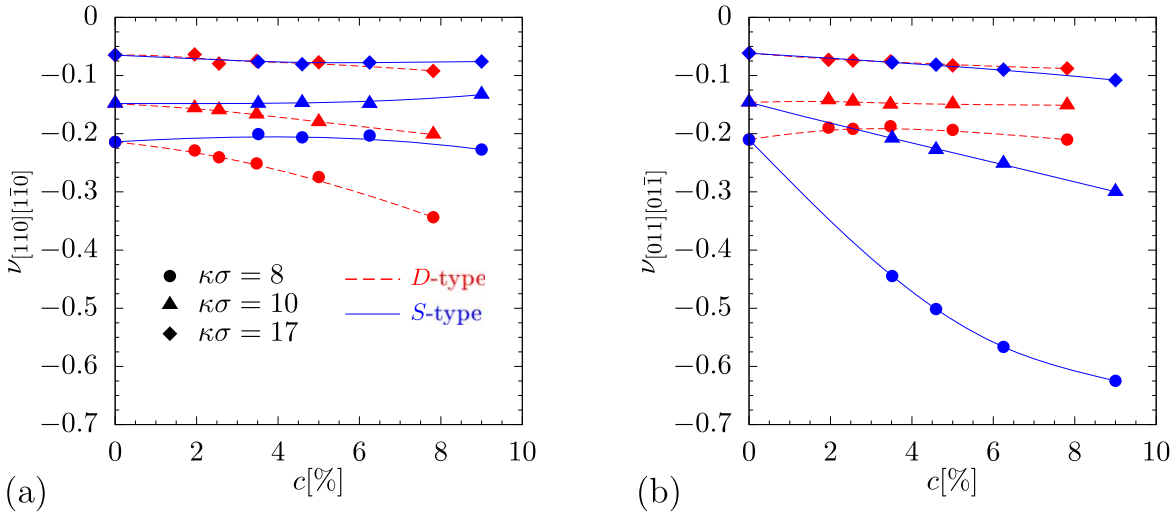

Figure 4. The Poissons ratio of Yukawa crystals with different types of nanochannels as a function of concentration: (a) the Poissons ratio in the $[110][1\bar{1}0]$-direction, (b) the Poissons ratio in the $[011][01\bar{1}]$-direction. (In this paper, we use the Miller indices for denoting both the direction of applied stress and the direction of measured response to the stress.) In both figures, lines are drawn to guide the eyes.

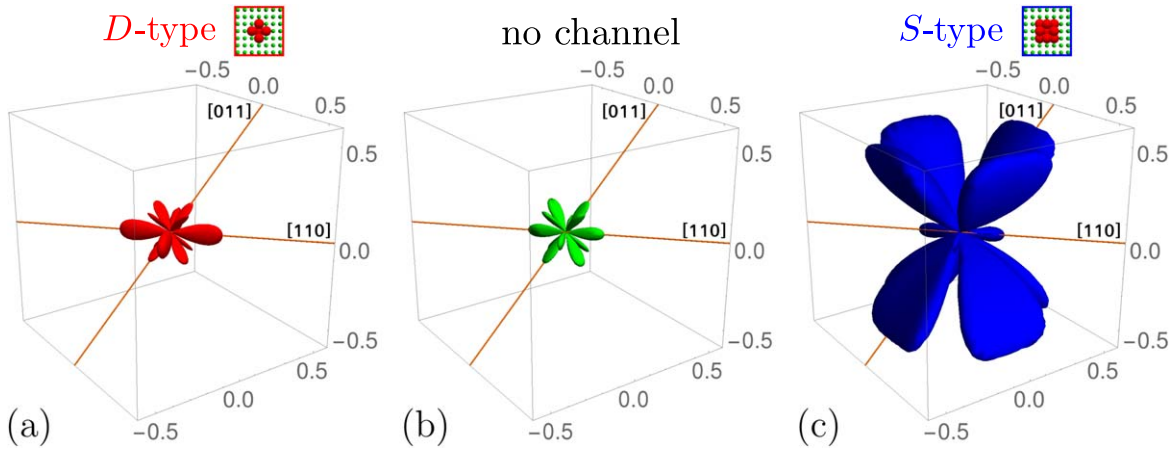

Figure 5. The absolute value of minimal negative Poissons ratio in all crystallographic directions of the Yukawa systems at $\kappa\sigma = 8$: (a) with nanochannels D-type for $c = 7.81\%$; (b) no nanochannels; (c) with nanochannels S-type for $c = 9\%$.

figure 5 one can see how the type of the nanochannel affects the Poisson's ratio in all crystallographic directions, compared to the Yukawa system without the nanochannel (figure 5(b)). It is worth to stress that, for the D-type channel, the decrease of Poisson's ratio in the $[110][1\bar{1}0]$-direction is accompanied by its increase in the $[011][01\bar{1}]$-direction (figure 5(a)). An opposite situation is observed for the S-type channel (figure 5(c)).

In order to estimate the changes of the auxetic properties (due to the presence of nanochannels) for the whole system, the degree of auxeticity [54] equation (6) has been calculated for each of the studied systems. Figure 6 presents χ as a function of concentration for both systems at various screening lengths. It can be concluded that S-type channel systems exhibit significantly stronger auxetic properties over the D-type channel systems (at $\kappa\sigma = 8$). However, along with the decrease of the screening length, this difference becomes less significant and is negligible at $\kappa\sigma = 17$. It disappears completely in the limiting case of hard sphere system, i.e. for $\kappa\sigma \to \infty$.

4. Conclusions

This work is an extension of the study of elastic properties of nanocomposite models based on structural modifications at the molecular level [50, 51, 55]. Here, we present the idea of modifications of the diameter of inclusions in the form of two types of nanochannels for the example of Yukawa crystals. The present study indicates that such modifications lead to a new possibility of selective enhancement or reduction of auxeticity of nanocomposite models.

Elastic properties of Yukawa crystals with two nanochannels of different diameters oriented in the [001]-direction have been evaluated by Monte Carlo simulations in the *NpT* ensemble. The present studies show that, depending on the nanochannel diameter, one can control (enhance or reduce) auxetic properties of the system in selected crystallographic directions ($[110][1\bar{1}0]$ and $[011][01\bar{1}]$). In particular, the introduction of nanochannels of S-type into Yukawa crystal allows one to decrease the Poisson's ratio of the system in the

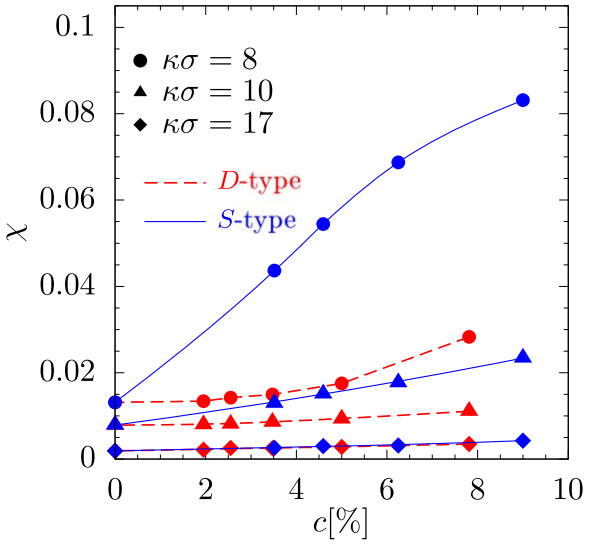

Figure 6. Auxeticity degree of Yukawa crystals with different types of nanochannels as a function of concentration of the 'channel' particles in the system. Lines are drawn to guide the eyes.

$[011][01\bar{1}]$-direction from $-0.214(9)$ (system without channel at $\kappa\sigma = 8$) to $-0.625(44)$. In turn, in the case of nanochannels of D-type, the Poisson's ratio of the system in the $[110][1\bar{1}0]$-direction changes its value from $-0.214(9)$ (system without channel at $\kappa\sigma = 8$) to $-0.344(49)$. It should be stressed that both types of nanochannels are introduced in the system in the [001]-direction but the enhancements of auxeticity are achieved in different crystallographic directions. This new effect appears due to the diameter modification of the inclusions that leads to different types of channels.

It is particularly noteworthy that the introduction of the S-type nanochannels into the system results in much greater amplification of auxeticity in the system (characterized by the auxeticity degree) compared to systems with D-type nanochannels. In addition, it is worth to mention that the Poisson's ratio of the system can be changed from $-0.061(9)$ (system without channel at $\kappa\sigma = 17$) to $-0.625(44)$ (system with D-type channel at $\kappa\sigma = 8$) due to different types of nanochannels and variation of such parameters as the inverse screening length and the concentration of the 'channel' particles in the system.

We believe that the results of this work have a general character and will be interesting not only from a theoretical point of view (in the sense of looking for basic mechanisms leading to auxetic behavior of the system) but also for researchers working on construction of composites as well as nanocomposites with special elastic properties.

Acknowledgments

The authors are grateful to MSc. Eng. Krzysztof Hyżorek for discussions and technical help in manuscript preparation. This work was supported by the grant 2017/27/B/ST3/02955 of the National Science Centre, Poland. The computations were partially performed at Poznań Supercomputing and Networking Center (PCSS).

ORCID iDs

Konstantin V Tretiakov https://orcid.org/0000-0003-4620-2807

References

[1] Evans K E, Nkansah M A, Hutchinson I J and Rogers S C 1991 Molecular network design *Nature* **353** 124
[2] Baughman R H 2003 Avoiding the shrink *Nature* **425** 667
[3] Xie P and Zhang R 2005 Liquid crystal elastomers, networks and gels: advanced smart materials *J. Mater. Chem.* **15** 2529–50
[4] Song Y, Wei W and Qu X 2011 Colorimetric biosensing using smart materials *Adv. Mater.* **23** 4215–36
[5] Hu J, Meng H, Li G and Ibekwe S 2012 A review of stimuli-responsive polymers for smart textile applications *Smart Mater. Struct.* **21** 053001
[6] Grima J N and Caruana-Gauci R 2012 Mechanical metamaterials materials that push back *Nat. Mater.* **11** 565–6
[7] White E M, Yatvin J, Grubbs J B, Bilbrey J A and Locklin J 2013 Advances in smart materials: stimuli-responsive hydrogel thin films *J. Polym. Sci.* B **51** 1084–99
[8] Liu Y, Du H, Liu L and Leng J 2014 Shape memory polymers and their composites in aerospace applications: a review *Smart Mater. Struct.* **23** 023001
[9] Barbarino S, Saavedra Flores E I, Dayyani I and Friswell M I 2014 A review on shape memory alloys with applications to morphing aircraft *Smart Mater. Struct.* **23** 063001
[10] Lim T C 2015 *Auxetic Materials and Structures* (Berlin: Springer)
[11] Lakes R S 2017 *Ann. Rev. Mater. Res.* **47** 63–81
[12] Duncan O, Shepherd T, Moroney C, Foster L, Venkatraman P D, Winwood K, Allen T and Alderson A 2018 *Appl. Sci.* **8** 941
[13] Landau L D and Lifshitz E M 1986 *Theory of Elasticity* (London: Pergamon)
[14] Lakes R S 1987 Foam structures with a negative Poisson's ratio *Science* **235** 1038–40
[15] Wojciechowski K W 1989 Two-dimensional isotropic model with a negative Poisson ratio *Phys. Lett.* A **137** 60–4
[16] Milton G 1992 Composite materials with Poisson's ratios close to -1 *J. Mech. Phys. Solids* **40** 1105–37
[17] Liu Q 2006 *Literature Review: Materials with Negative Poisson's Ratios and Potential Applications to Aerospace and Defence* (Victoria, Australia: Defence Science and Technology Organisation)
[18] Ma Y, Scarpa F, Zhang D, Zhu B, Chen L and Hong J 2013 A nonlinear auxetic structural vibration damper with metal rubber particles *Smart Mater. Struct.* **22** 084012
[19] Mizzi L, Attard D, Casha A, Grima J N and Gatt R 2014 On the suitability of hexagonal honeycombs as stent geometries *Phys. Status Solidi* b **251** 328–37
[20] Mercieca L A S, Formosa C, Grima J N, Chockalingam N, Gatt R and Gatt A 2017 On the use of auxetics in footwear: investigating the effect of padding and padding material on forefoot pressure in high heels *Phys. Status Solidi* b **254** 1700528
[21] Allen T, Hewage T, Newton-Mann C, Wang W, Duncan O and Alderson A 2017 Fabrication of auxetic foam sheets for sports applications *Phys. Status Solidi* b **254** 1700596

[22] Bathurst R J and Rothenburg L 1988 Note on a random isotropic granular material with negative Poisson's ratio *Int. J. Eng. Sci.* **26** 373–83
[23] Bowick M, Cacciuto A, Thorleifsson G and Travesset A 2001 Universal negative Poisson ratio of self-avoiding fixed-connectivity membranes *Phys. Rev. Lett.* **87** 148103
[24] Tretiakov K V 2009 Negative Poisson's ratio of two-dimensional hard cyclic tetramers *J. Non-Cryst. Solids* **355** 1435–8
[25] Goldstein R V, Gorodtsov V A and Lisovenko D S 2013 Classification of cubic auxetics *Phys. Status Solidi* b **250** 2038–43
[26] Verma P, Shofner M L and Griffin A C 2014 Deconstructing the auxetic behavior of paper *Phys. Status Solidi* b **251** 289–96
[27] Chetcuti E, Ellul B, Manicaro E, Brincat J-P, Attard D, Gatt R and Grima J N 2014 Modeling auxetic foams through semi-rigid rotating triangles *Phys. Status Solidi* b **251** 297–306
[28] Pozniak A A and Wojciechowski K W 2014 Poisson's ratio of rectangular anti-chiral structures with size dispersion of circular nodes *Phys. Status Solidi* b **251** 367–74
[29] Krasavin V V and Krasavin A V 2014 Auxetic properties of cubic metal single crystals *Phys. Status Solidi* b **251** 2314–20
[30] Ho D T, Kim H, Kwon S-Y and Kim S Y 2015 Auxeticity of face-centered cubic metal (001) nanoplates *Phys. Status Solidi* b **252** 1492–501
[31] Mizzi L, Gatt R and Grima J N 2015 Non-porous grooved single-material auxetics *Phys. Status Solidi* b **252** 1559–64
[32] Ha C S, Plesha M E and Lakes R S 2016 Chiral three-dimensional isotropic lattices with negative Poisson's ratio *Phys. Status Solidi* b **253** 1243–51
[33] Alderson K, Nazaré S and Alderson A 2016 Large-scale extrusion of auxetic polypropylene fibre *Phys. Status Solidi* b **253** 1279–87
[34] Desmoulins A, Zelhofer A J and Kochmann D M 2016 Auxeticity in truss networks and the role of bending versus stretching deformation *Smart Mater. Struct.* **25** 054004
[35] Dudek K K, Gatt R, Mizzi L, Dudek M R, Attard D, Evans K E and Grima J N 2017 On the dynamics and control of mechanical properties of hierarchical rotating rigid unit auxetics *Sci. Rep.* **7** 46529
[36] Chen S and Ryu S C 2017 Design and characterization of rounded reentrant honeycomb patterns for lightweight and rigid auxetic structures *Smart Mater. Struct.* **24** 115026
[37] Dong L, Hou J and Li D 2018 Mechanical behaviors of hierarchical cellular structures with negative Poisson's ratio *J. Mater. Sci.* **53** 10209–16
[38] Li D, Yin J and Dong L 2018 Numerical analysis of a two-dimensional open cell topology with tunable Poisson's ratio from positive to negative *Phys. Status Solidi* **12** 1700374
[39] Strek T, Jopek H, Maruszewski B T and Nienartowicz M 2014 Computational analysis of sandwich-structured composites with an auxetic phase *Phys. Status Solidi* b **251** 354–66
[40] Verma P, Shofner M L, Lin A, Wagner K B and Griffin A C 2015 Inducing out-of-plane auxetic behavior in needle-punched nonwovens *Phys. Status Solidi* b **252** 1455–64
[41] Shufrin I, Pasternak E and Dyskin A V 2015 Hybrid materials with negative Poisson's ratio inclusions *Int. J. Eng. Sci.* **89** 100–20
[42] Zhou L, Jiang L and Hu H 2016 Auxetic composites made of 3d textile structure and polyurethane foam *Phys. Status Solidi* b **253** 1331–41
[43] Mohanraj H, Filho Ribeiro S L M, Panzera T H, Scarpa F, Farrow I R, Jones R, Davies-Smith A, Remillat C D L, Walters P and Peng H-X 2016 Hybrid auxetic foam and perforated plate composites for human body support *Phys. Status Solidi* b **253** 1378–86
[44] Pasternak E, Shufrin I and Dyskin A V 2016 Thermal stresses in hybrid materials with auxetic inclusions *Compos. Struct.* **138** 313–21
[45] Gorodtsov V A, Lisovenko D S and Lim T-C 2018 Three-layered plate exhibiting auxeticity based on stretching and bending modes *Compos. Struct.* **194** 643–51
[46] Strek T, Jopek H and Nienartowicz M 2015 Dynamic response of sandwich panels with auxetic cores *Phys. Status Solidi* b **252** 1540–50
[47] Jopek H and Strek T 2015 Thermal and structural dependence of auxetic properties of composite materials *Phys. Status Solidi* b **252** 1551–8
[48] Strek T, Jopek H and Idczak E 2016 Computational design of two-phase auxetic structures *Phys. Status Solidi* b **253** 1387–94
[49] Lisovenko D S, Baimova J A, Rysaeva L K, Gorodtsov V A, Rudskoy A I and Dmitriev S V 2016 Equilibrium diamond-like carbon nanostructures with cubic anisotropy: elastic properties *Phys. Status Solidi* b **253** 1295–302
[50] Tretiakov K V, Piglowski P M, Hyzorek K and Wojciechowski K W 2016 Enhanced auxeticity in Yukawa systems due to introduction of nanochannels in [001]-direction *Smart Mater. Struct.* **25** 054007
[51] Piglowski P M, Wojciechowski K W and Tretiakov K V 2016 Partial auxeticity induced by nanoslits in the Yukawa crystal *Phys. Status Solidi* **10** 566–9
[52] Bilski M and Wojciechowski K W 2016 Tailoring Poisson's ratio by introducing auxetic layers *Phys. Status Solidi* b **253** 1318–23
[53] Narojczyk J W, Kowalik M and Wojciechowski K W 2016 Influence of nanochannels on Poisson's ratio of degenerate crystal of hard dimers *Phys. Status Solidi* b **253** 1324–30
[54] Piglowski P M, Narojczyk J W, Wojciechowski K W and Tretiakov K V 2017 Auxeticity enhancement due to size polydispersity in fcc crystals of hard-core repulsive Yukawa particles *Soft Matter* **13** 7916–21
[55] Piglowski P M, Narojczyk J W, Poźniak A A, Wojciechowski K W and Tretiakov K V 2017 Auxeticity of Yukawa systems with nanolayers in the (111) crystallographic plane *Materials* **10** 1338
[56] Tan H, Yu L and Zhou Z 2017 Negative Poisson's ratio in non-porous smooth curve sheet *Phys. Status Solidi* B **254** 1600612
[57] Hoover Wm G and Hoover C G 2005 Searching for auxetics with DYNA3D and ParaDyn *Phys. Status Solidi* b **242** 585–94
[58] Grima J N, Zammit V, Gatt R, Alderson A and Evans K E 2007 Auxetic behaviour from rotating semi-rigid units *Phys. Status Solidi* b **244** 866–82
[59] Ravirala N, Alderson A and Alderson K L 2007 Interlocking hexagons model for auxetic behaviour *J. Mater. Sci.* **42** 7433–45
[60] Attard D and Grima J N 2008 Auxetic behaviour from rotating rhombi *Phys. Status Solidi* b **245** 2395–404
[61] Grima J N, Gatt R and Farrugia P S 2008 On the properties of auxetic meta-tetrachiral structures *Phys. Status Solidi* b **245** 511–20
[62] Shufrin I, Pasternak E and Dyskin A V 2016 Deformation analysis of reinforced-core auxetic assemblies by close-range photogrammetry *Phys. Status Solidi* b **253** 1342–58
[63] Goldstein R V, Gorodtsov V A, Lisovenko D S and Volkov M A 2017 Two-layered tubes from cubic crystals: auxetic tubes *Phys. Status Solidi* b **254** 1600815
[64] Alderson K L, Simkins V R, Coenen V L, Davies P J, Alderson A and Evans K E 2005 How to make auxetic fibre reinforced composites *Phys. Status Solidi* b **242** 509–18
[65] Airoldi A, Bettini P, Panichelli P, Oktem M F and Sala G 2015 Chiral topologies for composite morphing structures?: I.

Development of a chiral rib for deformable airfoils *Phys. Status Solidi* b **252** 1435–45
[66] Hou X and Hu H 2015 A novel 3d composite structure with tunable Poisson's ratio and stiffness *Phys. Status Solidi* b **252** 1565–74
[67] Bacigalupo A, Lepidi M, Gnecco G and Gambarotta L 2016 Optimal design of auxetic hexachiral metamaterials with local resonators *Smart Mater. Struct.* **25** 054009
[68] Fozdar D Y, Soman P, Lee J W, Han L H and Chen S C 2011 Three-dimensional polymer constructs exhibiting a tunable negative Poisson's ratio *Adv. Funct. Mater.* **21** 2712–20
[69] Chen Y Y, Li T T, Scarpa F and Wang L F 2017 Lattice metamaterials with mechanically tunable Poisson's ratio for vibration control *Phys. Rev. Appl.* **7** 024012
[70] van Blaaderen A, Ruel R and Wiltzius P 1997 Template-directed colloidal crystallization *Nature* **385** 321–4
[71] Van Saders B, Dshemuchadse J and Glotzer S C 2018 Strain fields in repulsive colloidal crystals *Phys. Rev. Mater.* **2** 063604
[72] Alexeev V L, Das S, Finegold D N and Asher S A 2004 Photonic crystal glucose-sensing material for noninvasive monitoring of glucose in tear fluid *Clin. Chem.* **50** 2353–60
[73] Talapin D V, Lee J S, Kovalenko M V and Shevchenko E V 2010 Prospects of colloidal nanocrystals for electronic and optoelectronic applications *Chem. Rev.* **110** 389–458
[74] Galisteo-López J, Ibisate M, Sapienza R, Froufe-Peérez L, Blanco A and López C 2011 Self-assembled photonic structures *Adv. Mater.* **23** 30–69
[75] Ren X, Shen J, Tran P, Ngo T D and Xie Y M 2018 Auxetic nail: design and experimental study *Compos. Struct.* **184** 288–98
[76] Tretiakov K V and Wojciechowski K W 2014 Partially auxetic behavior in fcc crystals of hard-core repulsive Yukawa particles *Phys. Status Solidi* b **251** 383–7
[77] Azhar F E, Baus M and Ryckaert J P 2000 Line of triple points for the hard-core Yukawa model: a computer simulation study *J. Chem. Phys.* **112** 5121–6
[78] Auer S and Frenkel D 2002 Crystallization of weakly charged colloidal spheres: a numerical study *J. Phys.: Condens. Matter* **14** 7667–80
[79] Hynninen A-P and Dijkstra M 2003 Phase diagrams of hard-core repulsive Yukawa particles *Phys. Rev.* E **68** 021407
[80] Hansen J P and McDonald I R 2006 *Theory of Simple Liquids* (Amsterdam: Academic)
[81] Colombo J and Dijkstra M 2011 Effect of quenched size polydispersity on the fluid–solid transition in charged colloidal suspensions *J. Chem. Phys.* **134** 154504
[82] Heinen M, Holmqvist P, Banchio A J and Nagele G 2011 Pair structure of the hard-sphere Yukawa fluid: an improved analytic method versus simulations, Rogers–Young scheme, and experiment *J. Chem. Phys.* **134** 044532
[83] van der Linden M N, van Blaaderen A and Dijkstra M 2013 Effect of size polydispersity on the crystal-fluid and crystal-glass transition in hard-core repulsive Yukawa systems *J. Chem. Phys.* **138** 114903
[84] Royall C P, Leunissen M E, Hynninen A P, Dijkstra M and van Blaaderen A 2006 Re-entrant melting and freezing in a model system of charged colloids *J. Chem. Phys.* **124** 244706
[85] Smallenburg F, Vutukuri H R, Imhof A, van Blaaderen A and Dijkstra M 2012 Self-assembly of colloidal particles into strings in a homogeneous external electric or magnetic field *J. Phys.: Condens. Matter* **24** 464113
[86] Demirors A F, Pillai P P, Kowalczyk B and Grzybowski B A 2013 Colloidal assembly directed by virtual magnetic moulds *Nature* **503** 99–103
[87] Parrinello M and Rahman A 1981 Polymorphic transitions in single crystals: a new molecular dynamics method *J. Appl. Phys.* **52** 7182–90
[88] Parrinello M and Rahman A 1982 Strain fluctuations and elastic constants *J. Chem. Phys.* **76** 2662–6
[89] Wojciechowski K W, Tretiakov K V and Kowalik M 2003 Elastic properties of dense solid phases of hard cyclic pentamers and heptamers in two dimensions *Phys. Rev.* E **67** 036121
[90] Tokmakova S P 2005 Stereographic projections of Poisson's ratio in auxetic crystals *Phys. Status Solidi* b **242** 721–9
[91] Allen M P and Tildesley D J 1987 *Computer Simulations of Liquids* (Oxford: Clarendon)